Arabian Journal for Science and Engineering (2019) 44:5839–5850
https://doi.org/10.1007/s13369-019-03738-5

RESEARCH ARTICLE - MECHANICAL ENGINEERING

Experimental Investigation and Modeling of Surface Finish in Argon-Assisted Electrical Discharge Machining Using Dimensional Analysis

Nishant K. Singh[1] · Yashvir Singh[2]

Received: 20 July 2018 / Accepted: 1 February 2019 / Published online: 14 February 2019

Abstract
This study investigates the use of argon gas-assisted electrical discharge machining (AGAEDM) of high carbon high chromium die steel. Compressed argon gas in die-sinking EDM under controlled conditions was used to evaluate the surface roughness (SR). The influence of process parameters, viz., discharge current, pulse-on time, duty cycle, tool rotation, and discharge gas pressure, on SR has been investigated as well. Analysis of variance was applied to determine the significant factors affecting SR. In the course of this investigation, a semi-empirical model has been developed to determine SR through dimensional analysis while applying the AGAEDM process. The experimental and predicted values, gathered through the semi-empirical model, have been found to be in accord with each other. The mean error between the predicted and the experimental values was less than 5%. A comparison was performed between the RSM and semi-empirical models. The semi-empirical model was found to predict responses most precisely as compared to RSM model. In this connection, surface morphology analysis has also been done by using a scanning electron microscope in the machined specimens. The energy-dispersive X-ray and X-ray diffraction examination were used to study the relocation of different elements and development of compounds on the surface of the machined specimen.

Keywords Perforated · Gas pressure · Tool rotation · Dimensional analysis · Model

1 Introduction

Electrical discharge machining (EDM) is a widely used non-conventional machining process which utilizes heat from sparks to remove material from a stiff and hard workpiece, which cannot be machined using conventional methods. The process is widely applied for the fabrication of molds, dies, automotive and aeronautical components [1]. One of the major challenges encountered during EDM is flushing of diffused particles from an inter-electrode gap. There can be arcing and short circuit when debris is accumulated in the gaps between electrodes. This reduces surface finish and surface integrity [2].

✉ Nishant K. Singh
nishant.singh78@gmail.com

[1] Department of Mechanical Engineering, Hindustan College of Science and Technology, Mathura, India

[2] Department of Mechanical Engineering, Sir Padampat Singhania University, Udaipur, Rajasthan, India

1.1 Literature Review with Aspects of Improved Machining Performance of EDM

For improved machining performance, unconventional approaches were mentioned in the literature, including different flushing techniques and with electrodes of various types and materials, such as solid, tubular, eccentric hole and bundled. Mohan et al. [3] studied the influence of tool rotation and volume percentage of SiC during EDM of Al–SiC metal matrix composite (MMC). Kuppan et al. [4] studied small deep hole EDM drilling. The results revealed that material removal rate (MRR) can be significantly affected by the rotation of electrode, peak current and duty cycle. Further investigation suggested that peak current and pulse duration have an intense influence on surface roughness (SR). Teimouri and Baseri [5] studied impelled action of tool rotations and different intensity of the magnetic field on the EDM process. They compared the machining performance of the conventional EDM and magnetic field-assisted rotary EDM with the same processing parameters. Abdulkareem et al. [6] carried out an experiment to know the effect of a

cryogenically cooled electrode on process responses during EDM of titanium alloy workpiece. Srivastava and Pandey [7] investigated the effect of an ultrasonic-assisted cryogenically cooled tool on the machinability of the EDM process. They also compared the process responses of this tool with the conventional electrode. Aliakbari and Baseri [8] conducted Taguchi-based design of experiments (DOE) to obtain the optimum process factors for rotary-assisted multi-hole electrode EDM. They also studied the effect of machining factors on SR, MRR, electrode wear ratio (EWR) and over-cut. Gu et al. [9] did a feasibility analysis of EDM of Ti6Al4V by using bunched electrode. They also did a comparative analysis on a cryogenically cooled electrode and traditionally used electrode on EDM process responses. They suggested that use of bundled electrode significantly enhanced the material removal by improving the flushing of machining zone. Yoshida et al. [10] studied the effect of supplying of oxygen gas in dielectric liquid in EDM operation. They observed that when oxygen is dissolved in dielectric liquid and supplied in electrodes gap, machining performance improves significantly. Singh and Pandey [11] studied the effect of air-assisted multi-hole tool electrodes during the machinability of EDM process. They found the application of air-assisted multi-hole tool improve the MRR and reduced the EWR with respect to solid rotary tool electrodes under same machining conditions.

1.2 Literature Review in the Correlation of Mathematical Model Development

In order to enhance the machinability of the EDM process, researchers experimented with several conventional, advanced algorithm and innovative approaches. Due to the complex and arbitrary nature of various processes and a large number of process factors, there is a need to evolve an optimum approach. Wang and Tsai [12] used dimensional analysis technique to determine SR in different workpiece materials. They considered the electrical and thermal properties of electrodes along with prominent process factors to attain the desired model. The model they developed was found to be in accord with the experimental results. Yahya and Manning [13] studied the parameters influencing MRR during the die-sinking EDM process. They identified significant factors through analysis of variance (ANOVA) in order to develop a mathematical model for MRR on the basis of dimensional analysis. Kumar and Khamba [14] studied ultrasonic-assisted EDM of titanium and developed a micro-model to determine MRR by using Buckingham π-theorem approach. Patil and Brahmankar [15] proposed a semi-empirical model to predict MRR in wire electric discharge machining (WEDM). They developed a model by nonlinear estimation technique together with dimensional analysis. Yahya et al. [16] compared the results of MRR obtained from dimensional analysis and from an artificial neural network (ANN) model with low gap current by the EDM process. Dave et al. [17] developed a semi-empirical model by applying Buckingham π-theorem to predict MRR in Inconel 718 through the orbital-assisted EDM. The model was based on thermo-physical properties of Inconel 718, machining and orbital parameters. Kumar et al. [18] applied response surface methodology (RSM) to conduct and analyze the effects of parameters in WEDM on MRR and over-cut for pure titanium. Further, they developed a model to predict MRR by Buckingham π-theorem. Bobbili et al. [19] carried out a comparative study on the WEDM of armor materials by dimensional analysis related to MRR and SR. They considered thermal diffusivity, latent heat of vaporization, pulse duration, discharge pressure and input power as input parameters to develop the semi-empirical model for MRR and SR. Kumar et al. [20] developed mathematical model to predict tool Wear rate (TWR) using dimensional analysis during powder mixed EDM of titanium alloys. The finding suggested that thermal conductivity of specimen notably affected the TWR during machining of cryogenically treated specimens. In another investigation, Kumar et al. [21] developed a mathematical model based on dimensional analysis to predict MRR during EDM of cryogenically treated titanium alloy. The validation results reveal that experimental and predicted values are in good agreement. Further, they performed microstructure analysis to know the migration of different elements on the surface of a machined workpiece.

1.3 Research Gaps and Novelty of this Study

- Based on the literature review, it can be observed that most of the research work focused on either dry or near-dry EDM. Besides this, no attempt has been observed from literature to take the benefits of supply of compressed gas in conventional die-sinking EDM process.
- Singh et al. 11, 28 in their prior experimental investigations have found the advantage of gas-assisted EDM as compared to rotary EDM in terms of MRR and EWR. However, no work has been reported on the use of statistical design of experiment methodology known as RSM for the performing the experiments. This will eventually bring out the main effect and significance of various parameters for the gas-assisted EDM process.
- From the literature review, one could not discover any plausible work on a mathematical model, based on thermo–mechanical properties, which would ensure a better surface finish in gas-assisted EDM.
- The semi-empirical models, developed previously, were mostly based on machining process factors, electrical, physical and thermal characteristics of the specimen.
- Development of the model while considering dielectric properties, such as discharge gas pressure and tool

rotation speed for additional investigation has not been addressed in the literature.

In view of the aforementioned issues, the objective of the present study is to investigate and develop a semi-empirical model to predict SR by applying compressed argon gas through the perforated rotary tool in die-sinking EDM. Response surface method (RSM), a design of experiment technique, is used to plan the experiments and to get the parameters that significantly affected the process response. Buckingham π theorem is applied to develop a semi-empirical model between process factors and response.

2 Experimental Work

2.1 Specimen and Tool Electrode Material

The test was conducted on high carbon, high chromium die steel using tubular copper as tool electrode. The workpiece of rectangular shape (20 × 15 × 15 mm) and hardness of 51HRC was used. Table 1 shows the chemical composition of the selected specimens.

A perforated tube as a tool electrode, made of copper, was used to make sure a smooth flow of high-velocity argon gas through the electrode. Copper has good electrical and thermal conductivity. In order to ensure the effective transfer of heat from the tooltip, a tool electrode having 8.35 mm diameter and 70 mm length was chosen. The perforated electrode is shown in Fig. 1a, and the attachment used during the experiment is shown in Fig. 1b.

Table 1 Work piece chemical composition in terms of weight (%)

Cr	C	Si	Mn	P	S	Fe
10.05	2.30	0.40	0.30	0.05	0.03	Rest

Table 2 Process factors with their levels

Factors	Levels				
	−2	−1	0	1	2
Discharge current (I_p) (A)	3	4	5	6	7
Pulse-on time (T_{on}) (μs)	100	200	300	400	500
Duty cycle (DC)	0.52	0.58	0.64	0.70	0.76
Tool rotation (rpm)	100	300	500	700	900
Gas pressure (AP) (mm Hg)	3	6	9	12	15

2.2 Experimental Procedure

The machining time for gas-assisted die-sinking EDM with perforated electrode was fixed at 15 min for each experiment. Hydrocarbon-based oil (Kerosene) was used as the dielectric medium. For the test experimentation, five controllable process parameters, viz., discharge current, pulse-on time, duty cycle, tool rotation speed, and gas pressure were selected. The value of these parameters was fixed on the basis of trials experimentation and machine capacity. Compressed argon gas has been used in die-sinking EDM operation to prevent the oxidation reaction, chances of fire and hazards during the machining operation.

Table 2 presents the machining parameters range used for the present work. The open circuit voltage was fixed at 60 V for all experiments. The machined specimens were cleaned with acetone. Surface roughness tester Mitutoyo (Model: SJ

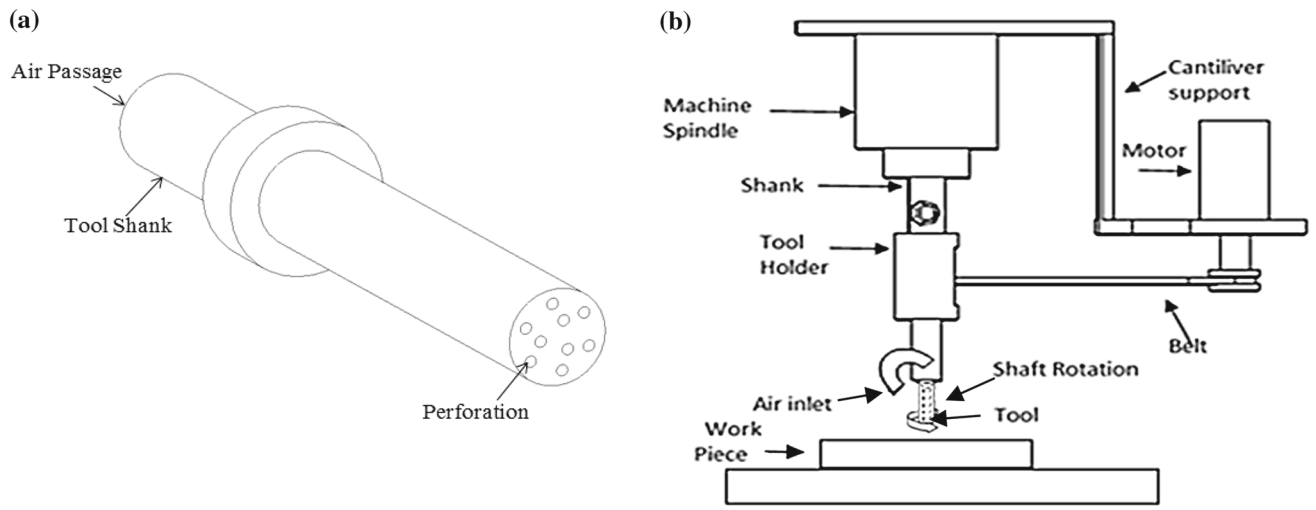

Fig. 1 Schematic diagram of **a** tool electrode **b** experiment setup mounted on EDM machine [11]

201P) was used to measure the surface finish of the machined specimen. In order to ensure an accurate machining time calculation, electronic timer (accuracy of 0.1 s) was used.

3 Analysis of Experimental Data

ANOVA was done to identify the principal parameters influencing SR during the AGAEDM process. The ANOVA of a second-order model has been presented in Table 3. For the model, the value of 'Prob > F' is found to be smaller than 0.05 (95% confidence). Hence, it is evident that the parameters in the model had a significant influence on the output response. The Eq. 1 represent the regression model of SR.

$$\begin{aligned} \mathrm{SR} = & -5.39 - (0.019 \times I_\mathrm{p}) - (0.0145 \times T_\mathrm{on}) \\ & + (15.9 \times \mathrm{DC}) + (0.000883 \times \mathrm{RPM}) \\ & + (1.16 \times \mathrm{GP}) + (0.000956 \times I_\mathrm{p} \times T_\mathrm{on}) \\ & + (0.0117 \times T_\mathrm{on} \times \mathrm{DC}) \\ & - (1.76 \times \mathrm{DC} \times \mathrm{GP}) \end{aligned} \quad (1)$$

3.1 Effects of Process Parameters on Surface Roughness

Figure 2 shows the main effect plots for SR. It can be inferred that SR increases with an enhancement in discharge current, duty cycle, and tool rotation. It was also noticed that SR comes down with an increase in pulse-on time. SR

Table 3 ANOVA table for SR

Source	DF	Seq. SS	MS	F	P	R^2	
Regression	7	5.334	0.762	50.03	0	0.9359	$F^{standard}_{(0.05,7,24);} = 2.87$
Linear	5	3.964					$F^{regression} > F^{standard}_{(0.05,7,24)}$
Interaction	2	1.370					$F^{standaed}_{(0.05,19,24);} = 2.91$
Residual error	24	0.365	0.015				$F^{lack\text{-}of\text{-}fit} < F^{standard}_{(0.05,19,24)}$
Lack-of-fit	19	0.332		2.68	0.139		Model is adequate and lack of fit is insignificant
Pure error	5	0.0015					
Total	31	0.7332					

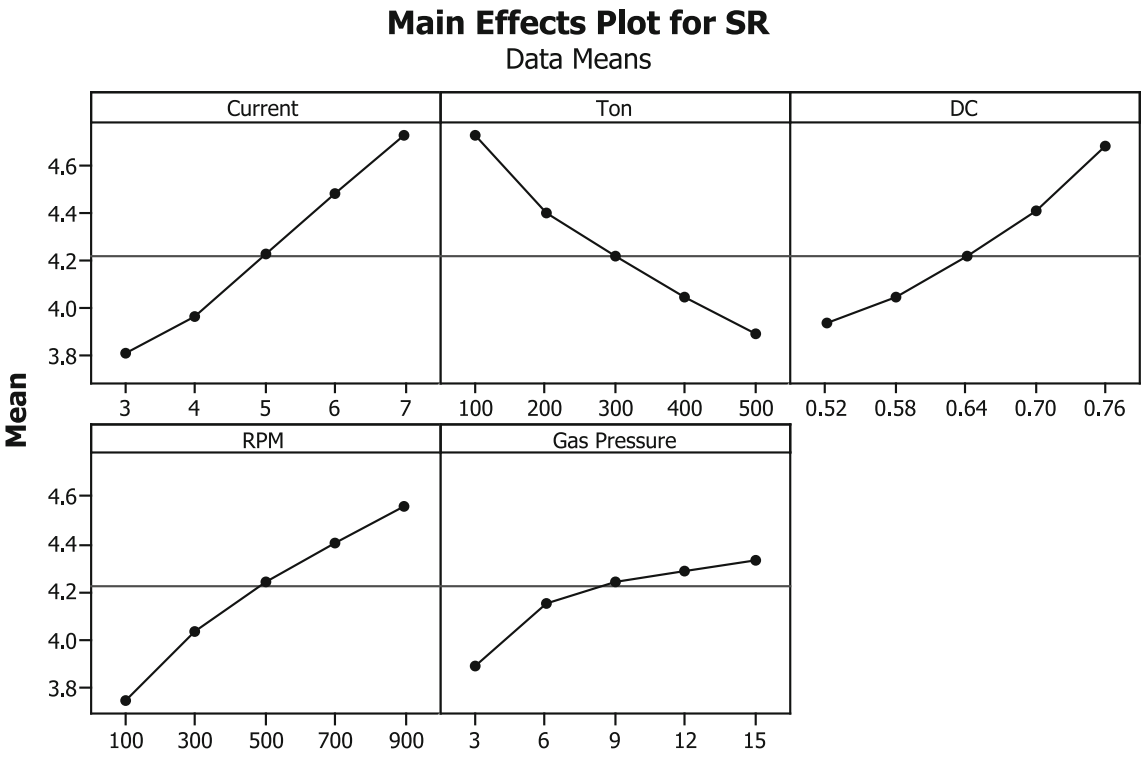

Fig. 2 Main effects for surface roughness of AGAEDM

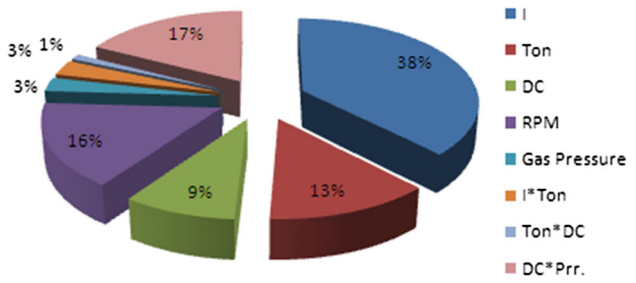

Fig. 3 Contribution (%) of each parameter on surface roughness for AGAEDM

shows an initial increase with discharge gas pressure and then decreases. It is probably due to the flushing efficiency of the process which improves with a rise in discharge gas pressure, leading to a reduction in SR. When the gas pressure is further increased, it resulted in low recast layer deposition. The carbon deposition is also minimum which is responsible for the reduced SR [22].

Figure 3 shows the contribution percentage of each parameter in the SR model. From the *pi*-chart, it can be observed that factors, significantly affecting SR, are discharge current, tool speed, pulse-on time and duty cycle. The discharge current is observed to be the most notable factor affecting the SR with a contribution of 38%, which is followed by tool speed, pulse-on time and duty cycle with a contribution of 16%, 13%, and 9%, respectively.

4 Dimensional Analyses for Assessing Surface Roughness During AGAEDM Process

The dimensional analysis is a method employed to obtain a certain set of information about a given phenomenon. With the dimensional analysis, one can get a complete set of dimensionless parameters [23]. The dimensional analysis method is basically used to reduce the complexity of a physical problem by reducing the number of factors, which may not significantly affect a given problem [12]. Table 4 shows the factors, symbol, value and the dimensions of physical quantities.

If the concerned physical problem has 'n' variables and if 'k' denotes fundamental dimensions, then dimensional analysis reduces the problem to only π-dimensionless terms. Usually, '$n - k$' equals the number of dimensionless π-terms that govern the problem. Any quantity either dimensional or non-dimensional constants in physical circumstance under consideration are known as a variable [23].

$$\text{Function:}\quad \text{SR} = f(I_\text{p}, T_\text{on}, \text{RPM}, \text{GP}, \text{DC}, K, \sigma, \rho, C_\text{p}, \theta) \tag{2}$$

In the present case, the rank of a matrix is five and there are 11 variables. Hence, according to Buckingham π-theorem, there are six π-terms. Accordingly, the dimension formula for the relation is:

$$\begin{aligned}&[L]^{k_1}[QT^{-1}]^{k_2}[T]^{k_3}[T^{-1}]^{k_4}\\ &\quad [ML^{-1}T^{-2}]^{k_5}[MLT^{-3}\theta^{-1}]^{k_7}[M^{-1}L^{-3}TQ^2]^{k_8}\\ &\quad [ML^{-3}]^{k_9}[L^2T^2\theta^{-1}]^{k_{10}}[\theta]^{k_{11}} = [M^0L^0T^0\theta^0Q^0]\end{aligned} \tag{3}$$

$$\begin{aligned}\text{SR} = &\left(\frac{k}{\rho c_p^{1.5}\theta^{0.5}}\right)(Z) \times \left(\frac{I\rho C_p^{1.5}}{k^{1.5}\sigma^{0.5}}\right)^{\alpha} \times \left(\frac{T_{on}\rho C_p^2\theta}{K}\right)^{\beta}\\ &\times \left(\frac{\text{RPMK}}{\rho C_\text{p}^2\theta}\right)^{\gamma} \times \left(\frac{\text{GP}}{\rho C_\text{P}\theta}\right)^{\delta} \times (\text{DC})^{\lambda}\end{aligned} \tag{4}$$

Table 4 Factors, symbol, value and dimension of physical quantities

Factors	Symbol	Value	Dimensions
Process parameters			
Current	Ip		$[QT^{-1}]$
Pulse-on time	T_on		$[T]$
Rotation	RPM		$[T^{-1}]$
Gas pressure	GP		$[ML^{-1}T^{-2}]$
Duty cycle	–		[1]
Material properties			
Thermal conductivity	K	$50\,W/m-K$	$[MLT^{-3}\theta^{-1}]$
Electrical conductivity	σ	$0.01824\,S/m$	$[M^{-1}L^{-3}TQ^2]$
Density	ρ	$7700\,Kg/m^3$	$[ML^{-3}]$
Sp. heat	C_p	$0.46\,Cal/S\,mole\,^\circ C$	$[L^2T^{-2}\theta^{-1}]$
Melting point	θ	$1421\,0^C$	$[\theta]$
Response			
Surface roughness	SR		$[L]$

Table 5 Precision of prediction model

Response	Mean error (ME)	Root-mean-square error (RMSE)	Average percentage error (ΔE %)
SR	0.0635	0.1274	4.35

Table 6 Validation of developed model of SR prediction

Exp. no.	Machining parameters				SR (μm)			Error (%)
	I	T_{on}	DC	RPM	GP	Exp.	Predicted	
1	7	300	0.58	500	12	4.87	4.70	3.40
2	4	100	0.64	300	9	4.31	4.13	4.17
3	5	200	0.52	100	6	2.65	2.55	3.77

where Z is the dimensionless constant and $\alpha, \beta, \gamma, \delta$ and λ are unidentified exponents. The nonlinear estimation method is used to determine the dimensionless constant and unknown exponents. The values of Z, α, β, γ, δ and λ are found to be 23207823.51, 0.1938, −0.1091, 0.3412, 0.0567 and 0.3538 respectively. The detailed methodology is thoroughly explained in Appendix ***A***. Equation (4) can be written in the following form:

$$\mathrm{SR} = (23207823.51) \times \left(\frac{I\rho C_{\mathrm{p}}^{1.5}}{k^{1.5}\sigma^{0.5}}\right)^{0.1938} \times \left(\frac{T_{\mathrm{on}}\rho C_{\mathrm{p}}^{2}\theta}{K}\right)^{-0.1091} \times \left(\frac{\mathrm{RPM\,K}}{\rho C_{\mathrm{p}}^{2}\theta}\right)^{0.3412} \times \left(\frac{\mathrm{GP}}{\rho C_{\mathrm{P}}\theta}\right)^{0.0567} \times (\mathrm{DC})^{0.3538} \quad (5)$$

The adequacy of the developed model was checked by the mean error (ME), root-mean-square error (RMSE) and average percentage error (ΔE%). The following equations were used for these analyses:

$$\mathrm{ME} = \frac{1}{n}\sum_{i=1}^{n}(X_{\mathrm{i}} - X) \quad (6)$$

$$\mathrm{RMSE} = \sqrt{\frac{1}{n}\sum_{i=1}^{n}(X_{\mathrm{i}} - X)^2} \quad (7)$$

$$\Delta E(\%) = \frac{1}{n}\sum_{i=1}^{n}(X_{\mathrm{i}} - X) \times 100 \quad (8)$$

where n is the total number of data, X_{i} is the value of measured data and X is the value, predicted by the semi-empirical model. The precision of the prediction model was estimated by using the mean error (ME), root-mean-square error (RMSE), average percentage error (ΔE%) and is listed in Table 5. From these values, it can be concluded that the developed model enables more accurate and precise prediction [17].

Three confirmation experiments were conducted under different parametric conditions to validate the proposed model. Details are presented in Table 6. It can be inferred from Table 6 that the percentage variation between experimental and predicted values are found to be less than 5%. Hence, the proposed model can predict SR during the AGAEDM process with good accuracy.

5 Results and Discussion

The experimental and predicted values, obtained through semi-empirical models, have been compared in the following Sections.

5.1 Influence of Process Factors on Surface Roughness During AGAEDM Process

The semi-empirical models, developed previously, were mostly based on machining process factors, electrical, physical and thermal characteristics of the specimen. Apart from the above-mentioned factors, in the present study, dielectric properties, such as discharge gas pressure and tool rotation speed were also considered for additional investigation. The comparative results of the RSM model, semi-empirical model, and experimental values are depicted in Fig. 4a–e. The results show a good agreement between experimental values and predicted values in the semi-empirical model. From Fig. 4, it can be concluded that the semi-empirical model enables more authentic and precise prediction in comparison of the RSM model. This model can be further applied to examine SR as well as other process responses.

The experimental and predicted values of SR during the AGAEDM process are presented in Fig. 5. The experimental results and model prediction values of SR during the AGAEDM process can be found to be in accord with one another. The average error between the model predictions and the experimental values can be found to be less than 5%. The contribution percentage of each factor and error on the

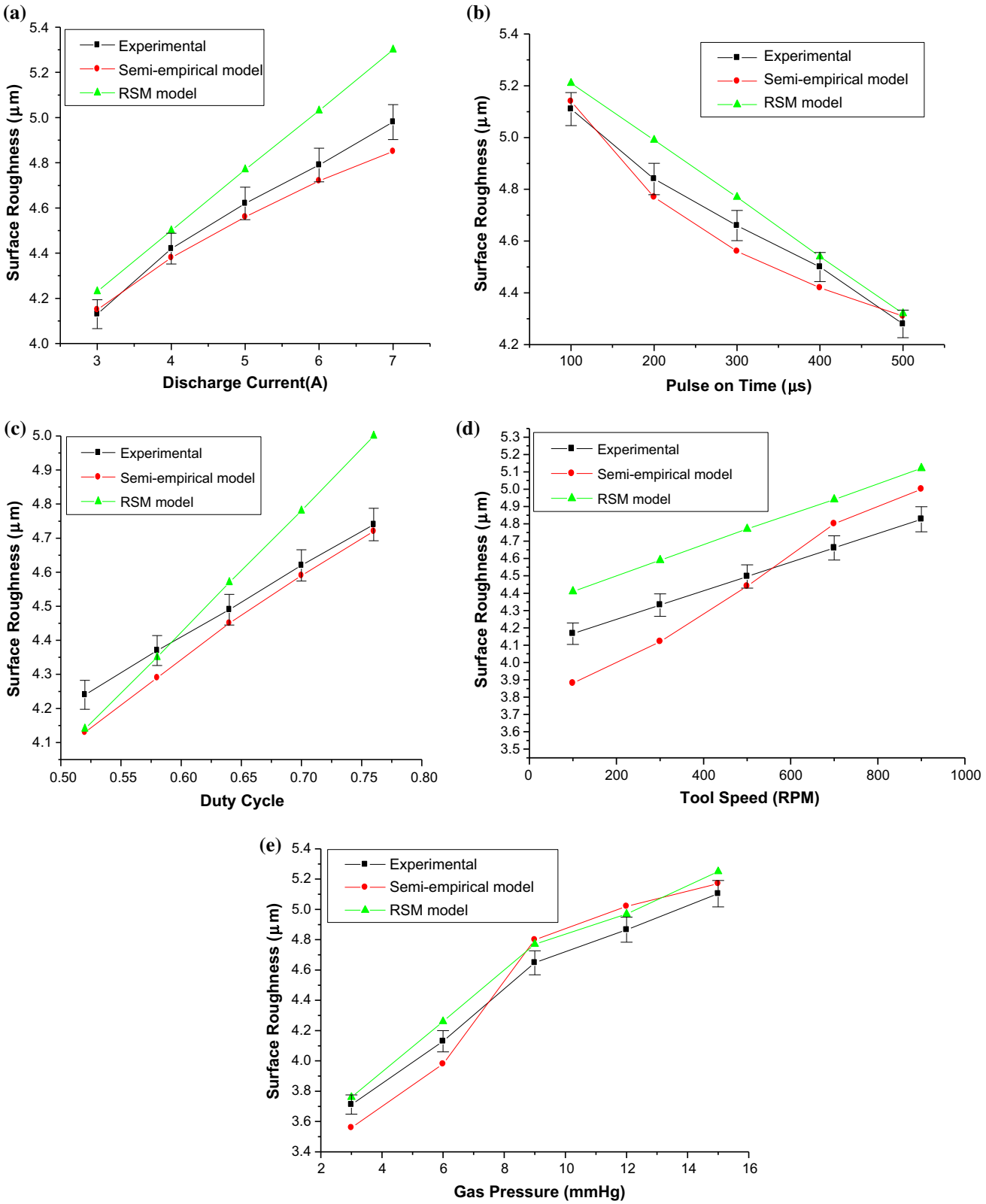

Fig. 4 Surface roughness values predicted by experimental and semi-empirical model for **a** discharge current **b** pulse-on time **c** duty cycle **d** tool speed **e** discharge gas pressure

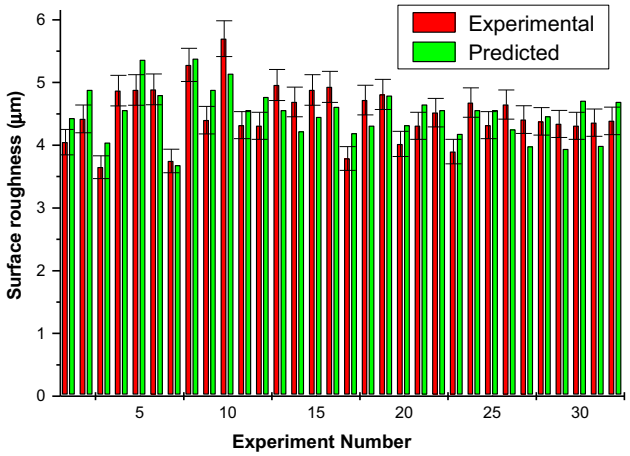

Fig. 5 Comparison of experimental results and model predicted value of surface roughness during AGAEDM

response, determined by the value of variance of error (V_e) and the sum of squares for regression as obtained from the ANOVA table [24], can be formulated as follows:

$$\Delta Y = t_{\alpha/2}, \mathrm{DF}\sqrt{V_e} \tag{9}$$

where ΔY stands for the error in response, the level of the confidence interval is denoted by α and is taken as 0.05. The variance of error of predicted process response is denoted by V_e. The calculated error is also indicated in Fig. 5 by using error bars.

6 Analysis of Surface Morphology

Scanning electron microscope (SEM) was used to look into the microstructural qualities of the machined specimens. The functional efficiency and characteristics of the machined surface were found to be adversely affected by the presence of surface cracks, recast white layer, micropores, deposition of carbon and other elements [25,26]. In the present study, the surface quality of the machined specimen was found to be significantly influenced by discharge current and pulse-on time. Four specimens, machined at lower and higher discharge current and pulse-on time, were selected for the surface analysis. The SEM images of the machined surface as illustrated in Figs. 6 and 7 established that large discharge craters are formed at higher discharge current and lower pulse-on time. The increase in discharge current from 3 to 7 A generates large discharge energy which causes greater depth on the machined specimen. An increase in spark energy develops larger craters, which deteriorate the surface quality [22]. From the SEM image referring to Fig. 7, one understands that the surface finish improves with a rise in pulse duration. In the rotary EDM process, as pulse duration increases, the width of the plasma channel increases as well, resulting in a reduction of energy density [27]. Thus, the size of the crater decreases; the smaller-sized eroded particles are flushed out easily from the electrode gap and improve the surface quality [26]. Further, from the SEM images, one can interpret that the large discharge energy develops surface cracks, which reduce the surface integrity of the machined samples. The compressed gas pressure plays an important role in material removal as well as in recast layer formation. There can be higher material removal and low recast layer formation when compressed gas is supplied at low pressure into the inter-electrode gap as it minimizes the effect of the short-circuit phenomenon [22]. The supply of compressed gas reduces the probability of recast layer formation due to the cooling obtained by compressed argon gas.

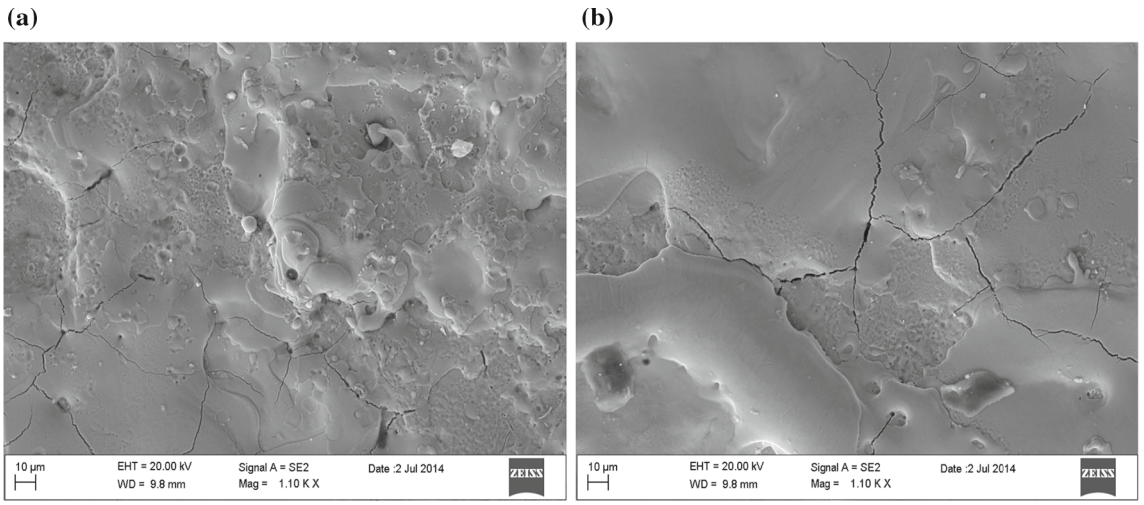

Fig. 6 SEM images of AGAEDM machined specimens at pulse-on time 300 µs, duty cycle 0.64, tool speed 500 rpm and discharged gas pressure 9 mm Hg **a** discharge current 3 A **b** discharge current 7 A

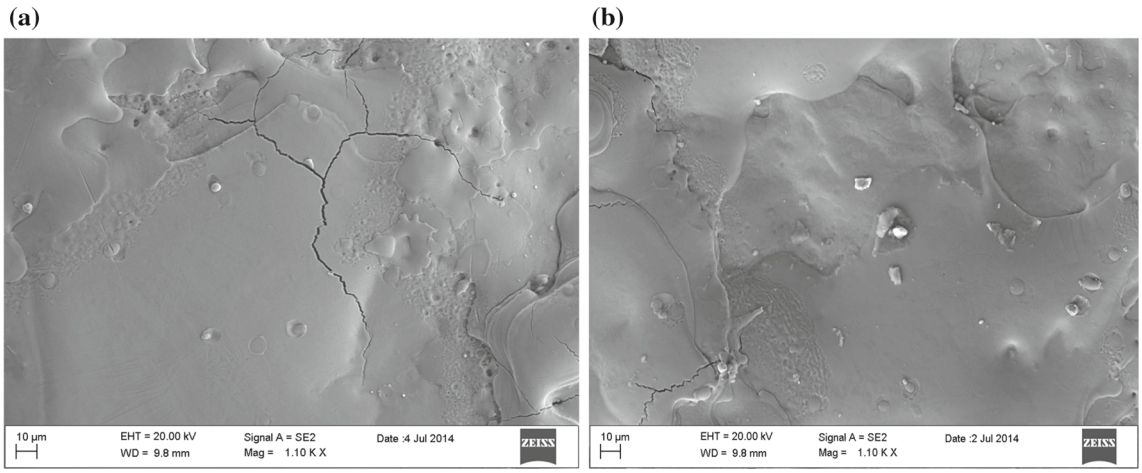

Fig. 7 SEM images of AGAEDM machined specimens at discharge current 5 A, duty cycle 0.64, tool speed 500 rpm and discharged gas pressure 9 mm Hg **a** pulse-on time 100 µs **b** pulse-on time 500 µs

6.1 Energy-Dispersive X-ray Analysis

Besides the SEM analysis, the composition of surface machined by AGAEDM process was examined by energy-dispersive X-ray (EDX) to know the chemical composition of the machined surface. Figure 8 shows the EDX of high carbon high chromium die steel specimen before machining. Figure 9 shows the EDX of the machined surface for the selected specimen, machined by the AGAEDM process. Fe, C, Cr, Si, Mn, P, and S are found to be the principal contents in the re-solidified layer. In the EDX analysis, Cu was not found in the re-solidified layer. This indicates that during the AGAEDM process, there is no visible transfer of tool material to the surface of the machined specimen. Further, from Fig. 9, it can be seen that there is a considerable rise in carbon proportion in the white layer with regard to the base material. There is a large deposition of carbon at the surface of the machined specimens, probably due to cracking of the hydrocarbon dielectric. Therefore, one may conclude that apart from melting and evaporation, material removal is also caused by decomposition. Similar observations were made by Mamalis et al. [22] and Srivastava et al. [28] with EDM of steel and Patel et al. [25] with EDM of ceramics.

6.2 X-ray Diffraction Analysis

The X-ray diffraction (XRD) examination was conducted to determine the chemical composition and phases on the surface of the machined specimen. The development of compounds like Fe_3C was observed on XRD pattern. It was probably due to migration of carbon as a result of dielectric cracking, interacts with iron and forms hard iron carbide (Fe_3C) compounds [20]. From Fig. 10, the formation of Fe_3C compounds may be seen at different 2 θ positions. Since Fe_3C is very hard and brittle, additionally it has high melting and boiling points. Thus, it requires high discharge energy for melting and evaporation, resulting in a reduced machining efficiency [20].

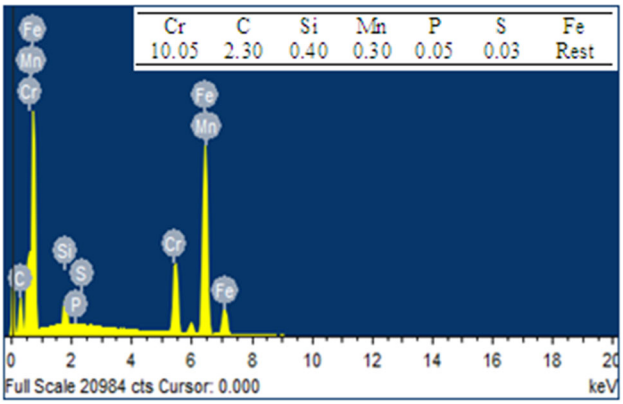

Fig. 8 EDX of the specimen surface before machining

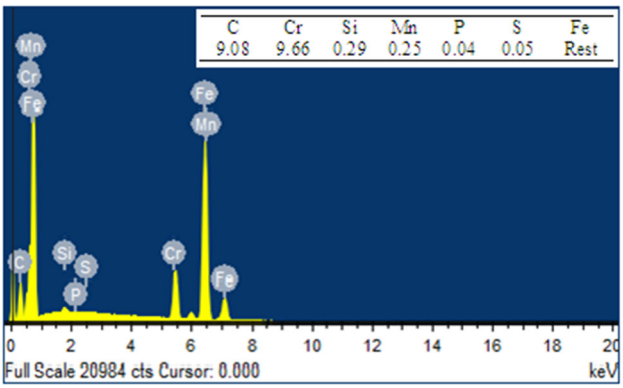

Fig. 9 EDX of the specimen surface after machining at a discharge gas pressure 9 mm Hg, discharge current of 5 A, duty cycle of 0.64, tool rotation of 500 rpm and pulse-on time of 300µs

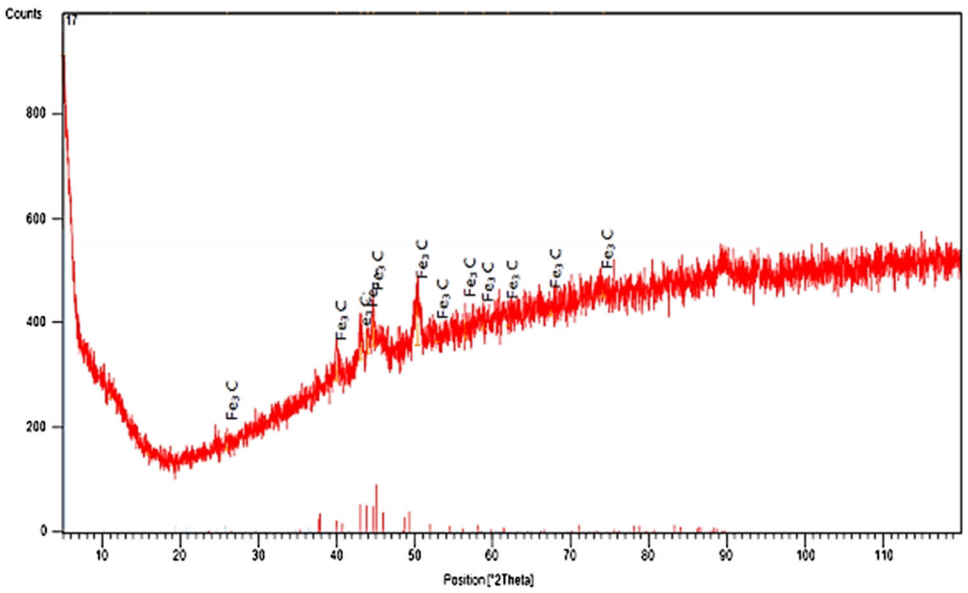

Fig. 10 XRD of the specimen surface after machining at a discharge gas pressure 9 mm Hg, discharge current of 5 A, duty cycle of 0.64, tool rotation of 500 rpm and pulse-on time of 300μs

Conclusions

In the present study, EDM of high carbon high chromium die steel was successfully conducted by the gas-assisted perforated rotary tool.

1. ANOVA was conducted to study the influence of various parameters on SR. The discharge current was found to be the most notable parameter influencing the SR, which was followed by tool speed, pulse-on time and duty cycle. The discharge gas pressure was found to be less significant parameters affecting the SR.
2. A semi-empirical model for SR was developed on the basis of dominant machining factors and thermo-physical properties of a specimen. The experimental and predicted value of the SR during the AGAEDM process was found to be in accord with one another. The mean error between the predicted and the experimental values was less than 5%.
3. The analysis of SEM images revealed that surface characteristics, viz., micropores, recast layers and surface cracks, increase at a higher discharge current and lower pulse- on time.
4. For validation of the semi-empirical model, confirmatory experiments were carried out. It can be inferred from the outcome that the proposed model can predict SR during the GAEDM process with good accuracy.
5. A comparison was done between the RSM and semi-empirical models to identify the most precise one between them. The semi-empirical model was found to predict responses most precisely as compared to the RSM model.

Appendix A: Derivation of the Dimensional Product

Required matrix, $\begin{bmatrix} 1 & -1 & 1 & 0 & 0 \\ 1 & -3 & -3 & 2 & 0 \\ -3 & 1 & 0 & -2 & 0 \\ -1 & 0 & 0 & -1 & 1 \\ 0 & 2 & 0 & 0 & 0 \end{bmatrix}$ Rank of matrix $= 5$

Now the dimension formula for the relation

$$\begin{aligned}&[L]^{k_1}[QT^{-1}]^{k_2}[T]^{k_3}[T^{-1}]^{k_4}[ML^{-1}T^{-2}]^{k_5}\\&\quad[MLT^{-3}\theta^{-1}]^{k_7}[M^{-1}L^{-3}TQ^2]^{k_8}[ML^{-3}]^{k_9}\\&\quad[L^2T^{-2}\theta^{-1}]^{k_{10}}\\&=[M^0L^0T^0\theta^0Q^0]\end{aligned} \tag{A1}$$

By equating power of the units

$$k_5 + k_7 - k_8 + k_9 = 0 \tag{A2}$$
$$k_1 - k_5 + k_7 - 3k_8 - 3k_9 + 2k_{10} \tag{A3}$$
$$-k_2 + k_3 - k_4 - 2k_5 - 3k_7 + k_8 - 2k_{10} = 0 \tag{A4}$$
$$-k_7 - k_{10} + k_{11} = 0 \tag{A5}$$
$$k_2 + 2k_8 = 0 \tag{A6}$$

The equations may be written in matrix form as,

$$Ak = c_1$$

$$A = \begin{bmatrix} 1 & -1 & 1 & 0 & 0 \\ 1 & -3 & -3 & 2 & 0 \\ -3 & 1 & 0 & -2 & 0 \\ -1 & 0 & 0 & -1 & 1 \\ 0 & 2 & 0 & 0 & 0 \end{bmatrix} \quad k = \begin{bmatrix} k_7 \\ k_8 \\ k_9 \\ k_{10} \\ k_{11} \end{bmatrix}$$

$$c_1 = [-1, 0, 1, 1.5, 0.5]^T$$

Table 7 Dimensions of model parameters

Dimensions	Model parameters										
	k_1 SR	k_2 I	k_3 T_{on}	k_4 RPM	k_5 GP	k_6 τ	k_7 K	k_8 σ	k_9 ρ	k_{10} C_p	k_{11} θ
M	0	0	0	0	1	0	1	−1	1	0	0
L	1	0	0	0	−1	0	1	−3	−3	2	0
T	0	−1	1	−1	−2	0	−3	1	0	−2	0
θ	0	0	0	0	0	0	−1	0	0	−1	1
Q	0	1	0	0	0	0	0	2	0	0	0

Then, assigning $k_1 = 1$ and k_2 to $k_6 = 0$ gives the following relation

$$\pi_1 = \frac{\mathrm{SR}\rho C_\mathrm{p}^{1.5}\theta^{0.5}}{K}\pi_2 = \frac{I\rho C_\mathrm{p}^{1.5}}{k^{1.5}\sigma^{0.5}}\pi_3 = \frac{T_\mathrm{on}\rho C_\mathrm{p}^2\theta}{K}$$
$$\pi_4 = \frac{\mathrm{RPM\,K}}{\rho C_\mathrm{p}^2\theta}\pi_5 = \frac{\mathrm{GP}}{\rho C_\mathrm{P}\theta}$$

We know that a parameter that is already dimensionless becomes a π-parameter all by itself. Hence, as the duty cycle is already dimensionless, it becomes π-parameter, i.e., π_6 [22]. The correlation between dimensionless π-terms may be written as (see Table 7):

$$\mathrm{SR} = \left(\frac{K}{\rho C_\mathrm{P}^{1.5}\theta^{0.5}}\right) \times Z\left(\frac{I\rho C_\mathrm{P}^{1.5}}{K^{1.5}\sigma^{0.5}}\right)^{\alpha} \times \left(\frac{T_\mathrm{on}\rho C_\mathrm{p}^2\theta}{K}\right)^{\beta} \times \left(\frac{\mathrm{RPM\,K}}{\rho C_\mathrm{P}^2\theta}\right)^{\gamma} \times \left(\frac{\mathrm{GP}}{\rho C_\mathrm{P}\theta}\right)^{\delta} (\mathrm{DC})^{\lambda} \quad \text{(A7)}$$

where Z is a dimensionless constant and α, β, γ, δ and λ are unidentified exponents. The nonlinear estimation method is used to determine the dimensionless constant and unknown exponents. The value of Z, α, β, γ, δ and λ is found to be 0.1838, −0.1091, −0.3312, −0.0457, −0.3238 and 47.17 respectively. Equation (A_8) can be formulated as (see Table 8):

$$\mathrm{SR} = (23207823.51) \times \left(\frac{I\rho C_\mathrm{p}^{1.5}}{k^{1.5}\sigma^{0.5}}\right)^{0.1938} \times \left(\frac{T_\mathrm{on}\rho C_\mathrm{p}^2\theta}{K}\right)^{-0.1091} \times \left(\frac{\mathrm{RPM\,K}}{\rho C_\mathrm{p}^2\theta}\right)^{0.3412} \times \left(\frac{\mathrm{GP}}{\rho C_\mathrm{P}\theta}\right)^{0.0567} \times (\mathrm{DC})^{0.3538} \quad \text{(A8)}$$

Table 8 Results of dimensional analysis

	Dimensions	π_1	π_2	π_3	π_4	π_5
k_1	SR	1	0	0	0	0
k_2	I	0	1	0	0	0
k_3	T_{on}	0	0	1	0	0
k_4	N	0	0	0	1	0
k_5	GP	0	0	0	0	1
k_7	K	−1	−1.5	−1	1	0
k_8	σ	0	0.5	0	0	0
k_9	ρ	1	1	1	−1	−1
k_{10}	C_p	1.5	1.5	2	−2	−1
k_{11}	θ	0.5	0	1	−1	−1

References

1. Ho, K.; Newman, S.: State of the art electrical discharge machining (EDM). Int. J. Mach. Tools Manuf. **43**, 1287–1300 (2003)
2. Singh, N.K.; Pandey, P.M.; Singh, K.K.; Sharma, M.K.: Steps towards green manufacturing through EDM process: a review. Cogent Eng. **3**, 1272662 (2016). 2016/12/31
3. Mohan, B.; Rajadurai, A.; Satyanarayana, K.G.: Effect of SiC and rotation of electrode on electric discharge machining of Al–SiC composite. J. Mater. Process. Technol. **124**, 297–304 (2002). 2002/06/20/
4. Kuppan, P.; Rajadurai, A.; Narayanan, S.: Influence of EDM process parameters in deep hole drilling of Inconel 718. Int. J. Adv. Manuf. Technol. **38**, 74–84 (2007)
5. Teimouri, R.; Baseri, H.: Effects of magnetic field and rotary tool on EDM performance. J. Manuf. Process. **14**, 316–322 (2012). 2012/08/01/
6. Abdulkareem, S.; Khan, A.A.; Konneh, M.: Reducing electrode wear ratio using cryogenic cooling during electrical discharge machining. Int. J. Adv. Manuf. Technol. **45**, 1146–1151 (2009)
7. Srivastava, V.; Pandey, P.M.: Effect of process parameters on the performance of EDM process with ultrasonic assisted cryogenically cooled electrode. J. Manuf. Process. **14**, 393–402 (2012). 2012/08/01/
8. Aliakbari, E.; Baseri, H.: Optimization of machining parameters in rotary EDM process by using the Taguchi method. Int. J. Adv. Manuf. Technol. **62**, 1041–1053 (2012)
9. Gu, L.; Li, L.; Zhao, W.; Rajurkar, K.P.: Electrical discharge machining of Ti6Al4V with a bundled electrode. Int. J. Mach. Tools Manuf. **53**, 100–106 (2012). 2012/02/01/
10. Yoshida, M.; Ishii, Y.; Ueda, T.: Study on electrical discharge machining for cemented carbide with non-flammable dielectric liquid: influence of form of oxygen supplied to dielectric liquid on machining. Proc. Inst. Mech. Eng. B J. Eng. Manuf. **232**, 568–577 (2017). 2018/03/01

11. Singh, N.K.; Pandey, P.M.; Singh, K.K.: EDM with an air-assisted multi-hole rotating tool. Mater. Manuf. Process. **31**, 1872–1878 (2016). 2016/10/25
12. Tsai, K.-M.; Wang, P.-J.: Semi-empirical model of surface finish on electrical discharge machining. Int. J. Mach. Tools Manuf. **41**, 1455–1477 (2001). 2001/08/01/
13. Yahya, A.; Manning, C.D.: Determination of material removal rate of an electro-discharge machine using dimensional analysis. J. Phys. D Appl. Phys. **37**, 1467 (2004)
14. Kumar, J.; Khamba, J.S.: Modeling the material removal rate in ultrasonic machining of titanium using dimensional analysis. Int. J. Adv. Manuf. Technol. **48**, 103–119 (2009)
15. Patil, N.G.; Brahmankar, P.K.: Determination of material removal rate in wire electro-discharge machining of metal matrix composites using dimensional analysis. Int. J. Adv. Manuf. Technol. **51**, 599–610 (2010)
16. Yahya, A.; Trias, A.; Erawan, M.A.; Nor Hisham, K.; Khalil, K.; Rahim, M.A.A.: Comparison studies of electrical discharge machining (EDM) process model for low gap current. Adv. Mater. Res. **433–440**, 650–654 (2012)
17. Dave, H.K.; Desai, K.P.; Raval, H.K.: Development of semi empirical model for predicting material removal rate during orbital electro discharge machining of Inconel 718. Int. J. Mach. Mach. Mater. **13**, 215–230 (2013)
18. Kumar, A.; Kumar, V.; Kumar, J.: Semi-empirical model on MRR and overcut in WEDM process of pure titanium using multi-objective desirability approach. J. Braz. Soc. Mech. Sci. Eng. **37**, 689–721 (2014)
19. Bobbili, R.; Madhu, V.; Gogia, A.K.: Modelling and analysis of material removal rate and surface roughness in wire-cut EDM of armour materials. Eng. Sci. Technol. Int. J. **18**, 664–668 (2015). 2015/12/01/
20. Kumar, S.; Singh, R.; Batish, A.; Singh, T.P.: Modeling the tool wear rate in powder mixed electro-discharge machining of titanium alloys using dimensional analysis of cryogenically treated electrodes and workpiece. Proc. Inst. Mech. Eng. E J. Process Mech. Eng. **231**, 271–282 (2015). 2017/04/01
21. Kumar, S.; Batish, A.; Singh, R.; Singh, T.P.: A mathematical model to predict material removal rate during electric discharge machining of cryogenically treated titanium alloys. Proc. Inst. Mech. Eng. B J. Eng. Manuf. **229**, 214–228 (2015)
22. Mamalis, A.G.; Vosniakos, G.C.; Vaxevanidis, N.M.; Prohászka, J.: Macroscopic and microscopic phenomena of electro-discharge machined steel surfaces: an experimental investigation. J. Mech. Work. Technol. **15**, 335–356 (1987). 1987/12/01/
23. Sonin, A.A.: "Dimensional analysis," Technical report, Massachusetts Institute of Technology (2001)
24. Srivastava, V.; Pandey, P.M.: Experimental investigation on electrical discharge machining process with ultrasonic-assisted cryogenically cooled electrode. Proc. Inst. Mech. Eng. B J. Eng. Manuf. **227**, 301–314 (2013). 2013/02/01
25. Patel, K.; Pandey, P.M.; Rao, P.V.: Study on machinability of Al2O3 ceramic composite in EDM using response surface methodology. J. Eng. Mater. Technol. **133**, 021004 (2011)
26. Singh, N.K.; Pandey, P.M.; Singh, K.K.: Experimental investigations into the performance of EDM using argon gas-assisted perforated electrodes. Mater. Manuf. Process. **32**, 940–951 (2017). 2017/07/04
27. Chattopadhyay, K.; Verma, S.; Satsangi, P.; Sharma, P.: Development of empirical model for different process parameters during rotary electrical discharge machining of copper-steel (EN-8) system. J. Mater. Process. Technol. **209**, 1454–1465 (2009)
28. Srivastava, V.; Pandey, P.M.: Statistical modeling and material removal mechanism of electrical discharge machining process with cryogenically cooled electrode. Proc. Mater. Sci. **5**, 2004–2013 (2014)